

## Cloud Water Contents and Hydrometeor Sizes During the FIRE-Arctic Clouds Experiment

**Matthew D. Shupe**

*Science and Technology Corporation /  
NOAA, Environmental Technology Laboratory, Boulder, Colorado*

**Taneil Uttal**

*NOAA, Environmental Technology Laboratory, Boulder, Colorado*

**Sergey Y. Matrosov**

*Cooperative Institute for Research in Environmental Sciences, University of Colorado /  
NOAA, Environmental Technology Laboratory, Boulder, Colorado*

**A. Shelby Frisch**

*Cooperative Institute for Research in the Atmosphere, Colorado State University /  
NOAA, Environmental Technology Laboratory, Boulder, Colorado*

*J. Geophys. Res., FIRE ACE Special Issue.*

Submitted: December 10, 1999. Revised: May 23, 2000.

**Abstract.** During the year-long Surface Heat Budget of the Arctic Experiment (1997-1998), the NOAA/Environmental Technology Laboratory operated a 35-GHz cloud radar and the DOE/Atmospheric Radiation Measurement Program operated a suite of radiometers at an ice station frozen into the drifting ice pack of the Arctic Ocean. The NASA/FIRE-Arctic Clouds Experiment took place during April-July, 1998, with the primary goal of investigating cloud microphysical, geometrical and radiative properties with aircraft and surface-based measurements. In this paper, retrieval techniques are utilized which combine the radar and radiometer measurements to compute height-dependent water contents and hydrometeor sizes for all-ice and all-liquid clouds. For the spring and early summer period, all-ice cloud retrievals showed a mean particle diameter of about 60  $\mu\text{m}$  and ice water contents up to 0.1  $\text{g}/\text{m}^3$ , with the maximum sizes and water contents at approximately 1/5 of the cloud depth from the cloud base. The all-liquid cloud retrievals had a mean effective particle radius of 7.4  $\mu\text{m}$ , liquid water contents up to 0.7  $\text{g}/\text{m}^3$ , and a mean particle concentration of 54  $\text{cm}^{-3}$ . Maximum retrieved liquid drop sizes, water contents and concentrations occurred at 3/5 of the cloud depth from the cloud base. As a measure of how representative the FIRE-ACE aircraft flight days were of the April-July months in general, retrieval statistics for flight-day clouds are compared to the mean retrieval statistics. From the retrieval perspective, the ice particle sizes and water contents on flight days were approximately 30% larger than the mean retrieved values for the April-July months. Retrieved liquid cloud parameters during flight days were all about 20% smaller. All-ice and/or all-liquid clouds acceptable for these retrieval techniques were observed about 34% of the time that clouds were present; at all other times mixed-phase clouds precluded the use of any retrieval technique.

## 1. Introduction

The microphysical properties of clouds strongly influence their radiative properties. Factors such as phase, hydrometeor size and the distribution of water mass in the cloud interplay to determine how each individual cloud will affect radiative heating profiles in the atmosphere [Curry, 1986; Curry and Ebert, 1992; Stephens *et al.*, 1990]. In situ aircraft measurements of cloud microphysics are useful, but are limited by relatively small sample volumes, restrictively short flight times, and by the fact that the aircraft itself may modify the cloud with complex airstreams and vortices as it samples. Current satellite technologies infer cloud properties with passive remote sensors, which have inherent limitations on providing vertically resolved information, face issues of sub-pixel variations [Rossow *et al.*, 1993], and have the considerable problems associated with detecting clouds over snow-covered surfaces. The difficulty in measuring cloud characteristics has resulted in a spatially and temporally limited observational data base, leading to a poor representation of clouds, and particularly Arctic clouds, in global climate models [Curry *et al.*, 1996].

In the last decade a set of interrelated techniques has been developed to determine microphysical properties of clouds by combining measurements from surface-based radars with infrared and/or microwave radiometer measurements. These techniques were applied to year-long radar and radiometer measurements taken from an ice camp deployed in the Arctic ocean in 1997-1998 as part of the Surface Heat Budget of the Arctic (SHEBA) experiment [Perovich *et al.*, 1999; Uttal *et al.*, 2000]. The analysis period covered by this paper coincides with the four-month NASA/FIRE-Arctic Clouds Experiment (ACE), which was a partner research program primarily focused on aircraft measurements during the spring and early

summer of 1998 [Curry *et al.*, 2000].

## 2. Instrumentation

The SHEBA radar is a 35-GHz (Ka-band) system which measures radar reflectivity, Doppler velocity, and the Doppler spectral width. It is a copy of the systems that were designed and built by the NOAA/Environmental Technology Laboratory (ETL) for the DOE/Atmospheric Radiation Measurement (ARM) Program, with minor modifications to accommodate the Arctic environment and mounting on a ship. This system was designed to run without full-time operators, in remote locations, and with a minimum of maintenance and oversight. The system points vertically and produces long-term and continuous profiles of radar parameters through clouds and light precipitation. The single-polarization system uses a low-peak-power, high-duty-cycle traveling wave tube amplifier (TWTA) transmitter, a high-gain antenna and pulse compression techniques. The pulse compression techniques make this radar particularly sensitive, with an estimated detection threshold of -47 dBZ at 5 km above ground level (AGL). In the Arctic, attenuation of the radar signal is seldom an issue, and comparisons with lidar data indicate that tenuous cirrus below the sensitivity threshold of the radar occur only about 15% of the time [Intrieri *et al.*, 2000]. Therefore, the vertical profiles of the SHEBA radar reflectivities are considered to be a fairly complete description of cloudiness, precipitation and diamond dust over the ice camp. The radar is described more fully by Moran *et al.* [1998]. Reflectivities measured by the radar provide the foundation for both the liquid and ice water retrievals that are discussed in section 3.

The Atmospheric Emitted Radiance Interferometer (AERI) [Revercomb *et al.*, 1993] measures the downward absolute infrared spectral radiance (in units of watts per square meter per steradian per wavenumber). The

spectral range of the AERI channel 1 is  $500 \text{ cm}^{-1}$  ( $20 \text{ }\mu\text{m}$ ) to  $3300 \text{ cm}^{-1}$  ( $3 \text{ }\mu\text{m}$ ), with a spectral resolution of  $1.0 \text{ cm}^{-1}$ . The instrument field-of-view is 1.3 degrees, and a calibrated sky radiance spectrum is produced approximately every 7.1 minutes. For the retrievals presented in this paper, the infrared brightness temperature is calculated from the average radiance over a  $25 \text{ cm}^{-1}$  band centered on  $900 \text{ cm}^{-1}$  ( $11.1 \text{ }\mu\text{m}$ ). During periods when the AERI was not operational, a Pyrometrics Corporation infrared thermometer (IRT), which measures the radiance between 9.6 and  $11.5 \text{ }\mu\text{m}$ , was used. The IRT has the disadvantage of a minimum measurable brightness temperature of  $-60 \text{ }^\circ\text{C}$ , which is often considerably warmer than the Arctic sky.

The microwave radiometer used at SHEBA is a Radiometrics WVR-1100 with receivers at 23.8 and 31.4 GHz. Brightness temperatures measured by the radiometer at these frequencies are used to derive the liquid water path (LWP) and the integrated water vapor amount in approximately two-minute intervals. Initial discrepancies between the radiometer-derived LWP and LWP estimates from aircraft in situ measurements have led to a reprocessing of the radiometer data. More recent data (compared to those used in the original ARM processing algorithm) on the dielectric constants of super-cooled water were incorporated into the retrieval, resulting in LWP values that are in better agreement with the in situ estimates. Uncertainty in the dielectric constants still exists, however, with retrieved LWP varying in different models by as much as 20% at  $-10^\circ\text{C}$  (Ed Westwater, personal communication). All radiometers discussed here were operated by the ARM program and data acquisition and calibration were done in accordance with ARM data standards.

### 3. Retrieval Techniques

There are a variety of radar-radiometer,

retrieval techniques for inferring cloud microphysics which utilize different combinations of radiances, Doppler velocities, radar reflectivities and radar spectral widths [Frisch *et al.*, 1995; Mace *et al.*, 1998; Matrosov, 1997; Sassen *et al.*, 1999]. These techniques have been discussed at length in the literature; the purpose of this section will be to summarize the salient points of the techniques that were utilized during the FIRE-ACE experiment. Liquid retrieval papers by Frisch *et al.* [1998, 2000a] and an ice retrieval paper by Matrosov [1999] will be cited frequently, and will hereafter be referred to as *F98*, *F00*, and *M99*, respectively.

#### 3.1. Liquid retrievals

The technique for determining liquid water content (LWC) from radar reflectivity and integrated liquid water path retrieved from microwave radiometer measurements was first presented by Frisch *et al.* [1995], and developed further in *F98*, to show that retrieval of the water profile does not depend on a lognormal droplet distribution assumption and that the method is independent of radar calibration errors. This retrieval is based on the assumptions that both cloud droplet concentration and the width of the particle size distribution are constant with height. Using these assumptions, it is possible to write the relationship between liquid water content, LWC, and radar reflectivity,  $Z$ , as

$$LWC(h) = \frac{0.52\rho_w}{k} N^{1/2} Z(h)^{1/2} \quad (1)$$

where  $h$  is the height coordinate,  $\rho_w$  is the density of water in  $\text{g/cm}^3$ ,  $k$  is a constant relating the sixth and third moments of the droplet distribution,  $N$  is the assumed droplet concentration in  $\text{cm}^{-3}$ , reflectivity is in units of  $\text{m}^3$ , and LWC is in units of  $\text{g/m}^3$ . Liquid water path, LWP, can then be written as

$$\begin{aligned}
 LWP &= \sum_{h=1}^M LWC_h \Delta h \\
 &= \frac{0.52\rho_w}{k} N^{1/2} \sum_{h=1}^M Z(h)^{1/2} \Delta h, \quad (2)
 \end{aligned}$$

where  $\Delta h$  is the radar's vertical resolution, and the summation is over the total cloud thickness. Solving (2) for  $N^{1/2}$  and substituting into (1) yields an equation for LWC in terms of reflectivity and integrated liquid water path:

$$LWC(h) = LWP \frac{Z(h)^{1/2}}{\sum_{h=1}^M Z(h)^{1/2} \Delta h}, \quad (3)$$

where LWP is retrieved from measurements taken by the microwave radiometer. Using radar, radiometer and in situ aircraft measurements from the ARM Cloud and Radiation Test Bed site in Oklahoma, *Frisch et al.* [2000b] showed that the standard error of estimate for LWC obtained from (3) is about  $0.03 \text{ g/m}^3$ .

The droplet effective radius ( $R_e$ ) retrieval technique described in *F00* is independent of the LWC retrieval; therefore, different assumptions regarding particle concentration are applied. This retrieval is based on an empirical relationship between concentration and calculated radar reflectivity that was derived from a set of particle size spectra measured by an airborne Particle Measuring Systems (PMS) Forward Scattering Spectrometer Probe (FSSP-100). To make the *F00* technique specific to Arctic clouds, FSSP measurements made during the FIRE-ACE experiment from both the University of Washington (UW) Convair 580 and the National Center for Atmospheric Research (NCAR) C-130 were used in place of data collected in Oklahoma as described in *F00*. In situ data for developing this relationship were only considered when the total concentration of

liquid size particles measured by the FSSP was greater than  $10 \text{ cm}^{-3}$  and the total concentration of particles larger than about  $50 \mu\text{m}$  (measured by a PMS 1D-C on the UW aircraft and a PMS OAP-260X on the NCAR aircraft) was less than  $1 \text{ L}^{-1}$ . As described in *F00*, the concentration and reflectivity data were fit to yield a value of  $N$ , in 1-dBZ bin widths, that minimized the standard deviation in  $R_e$  using the relationship

$$R_e = 0.5 \frac{Z^{1/6}}{N^{1/6}} e^{-0.5\sigma^2}, \quad (4)$$

where  $\sigma$  is the logarithmic spread of the droplet size distribution. Based on the FIRE-ACE in situ data mentioned above,  $\sigma$  is  $0.34 \pm 0.09$ ; therefore, a value of 0.34 was used for all retrievals discussed here. This value of  $\sigma$  demonstrates a slight change from the *F00* value of 0.32. The empirical N-dBZ relationship (with  $Ze$  in units of dBZ) derived via the *F00* technique is:

$$\begin{aligned}
 N(Ze) &= 122.19 + 3.67(Ze) + 0.100(Ze)^2 \\
 &\quad + 0.002(Ze)^3 + 0.000014(Ze)^4. \quad (5)
 \end{aligned}$$

The coefficients of this relationship differ from those of the *F00* relationship due to the lower concentrations measured during FIRE-ACE. Effective radius is calculated from radar reflectivity by substituting (5) into (4).

The relationship (5) was fit to radar reflectivities between -53 and -10 dBZ since there were few FSSP size spectra yielding theoretical reflectivities outside these bounds. This range of reflectivities covered most non-precipitating liquid clouds observed during the April through July time period, however, to allow for a slightly larger range of reflectivities, (5) was extended to cover the interval from -60 to 0 dBZ. These reflectivity limits correspond to similar range limits in concentration ( $10\text{-}120 \text{ cm}^{-3}$ ) and

droplet effective radius (3-21  $\mu\text{m}$ ). The standard deviation of (5) was approximately  $15\text{ cm}^{-3}$  while the reflectivity-dependent standard deviation of (4) incorporating the values of (5) was generally between 0.5 - 1.5  $\mu\text{m}$ .

A three-hour period from 6:00 to 9:00 GMT on June 4, 1998 demonstrates the liquid cloud retrieval products. This time period consisted of a fairly stable stratus layer with cloud top near 700 m. Radar reflectivity, the key radar measurable for these retrievals, is shown in Figure 1a, retrieved LWC is shown in Figure 1b, and retrieved  $R_e$  is shown in Figure

1c. Since estimates of LWP from the microwave radiometer data are not affected by ice layers, the liquid retrievals can be applied to cases when ice and liquid are in the same vertical column but in separate cloud layers, for instance, high level cirrus above a low liquid stratus cloud. In these cases, such as the one described in Section 4, the retrieval is performed only through the depth of the low-altitude cloud which is presumed to contain all of the observed liquid. The liquid cloud retrieval techniques are also applicable when the liquid is distributed through multiple, all-liquid layers.

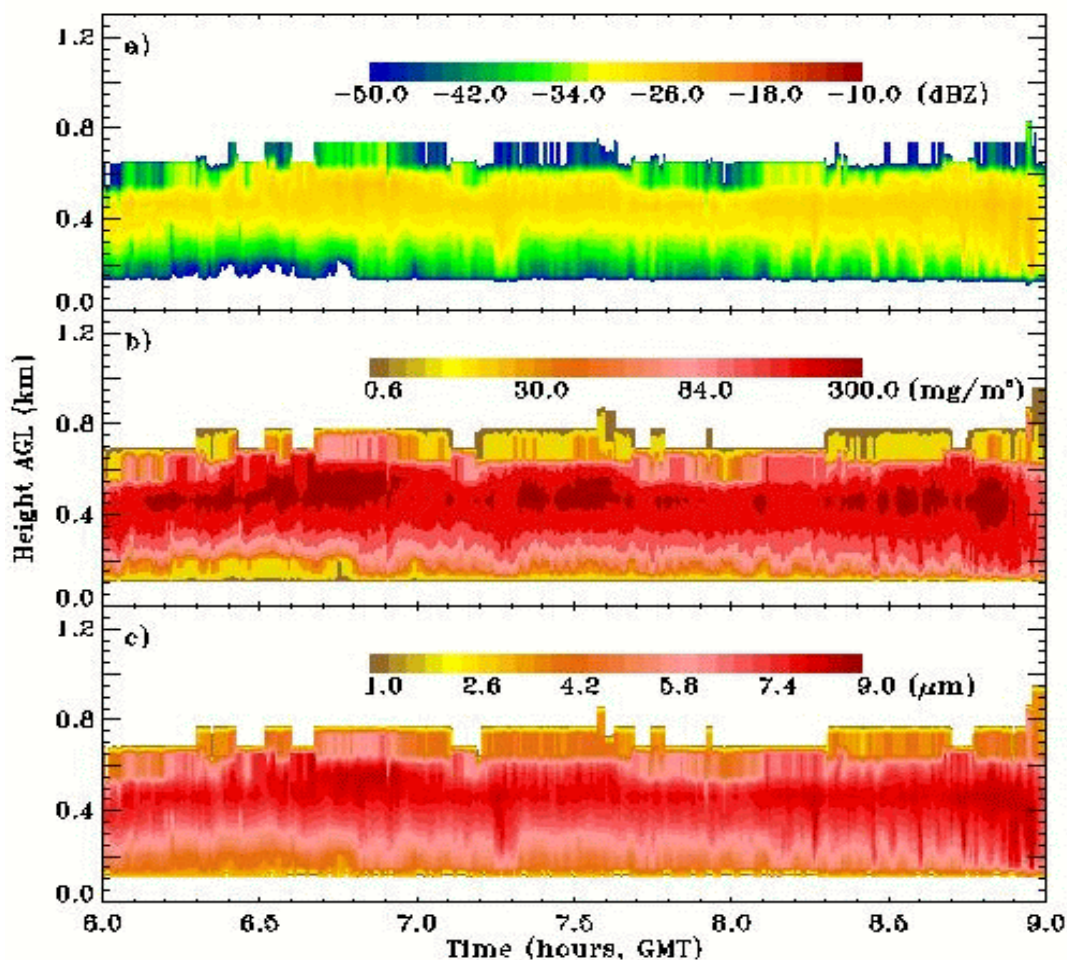


**Figure 1.** Time-height contours for June 4, 1998 of (a) radar reflectivity, (b) retrieved liquid water content, and (c) retrieved mean droplet radius.

### 3.2. Ice retrievals

A number of related techniques have been developed to determine ice-cloud water contents and particle sizes. *Matrosov et al.* [1992] used brightness temperatures from an IR radiometer (10-11.4  $\mu\text{m}$ ) and radar reflectivities to determine ice water path (IWP) and a layer mean particle size integrated over the cloud depth. The technique was expanded in *Matrosov et al.* [1994, 1997] by incorporating vertical Doppler velocities, so that profiles of ice water contents and particle sizes could be retrieved, rather than just layer-averaged quantities. During the SHEBA experiment, a combination of small but continuous shifts in the pack ice, and the pitch of the ship, resulted in misalignments in the radar antenna which introduced some contamination of the vertical velocities with a component from the horizontal winds. As a result the technique described in *Matrosov et al.* [1997] could not be applied. Therefore, in this paper, a third technique described by *M99* based on tuned regressions between reflectivity and cloud parameters is utilized so that profiles of IWC and particles sizes can be determined without Doppler information.

Over the years, a number of empirical power-law regressions have been proposed for relating ice water content (IWC) and radar reflectivity [*Atlas et al.*, 1995; *Liao and Sassen*, 1994; *Matrosov*, 1997; *Sassen*, 1987; *Sassen and Liao*, 1996] using equations of the form

$$IWC = aZ^b. \quad (6)$$

A wide range of “a” and “b” coefficients have been determined, often from aircraft data, for varying cloud conditions and geographical locations. The coefficients have varied enough to cause large differences in resulting IWC values [*Matrosov*, 1997], demonstrating the inaccuracies involved in applying any single

regression to data sets that include the diversity of cloud conditions that might be introduced by season, cloud altitude, or air mass characteristics. The “tuned regression” technique described in *M99* utilizes (6) but determines unique coefficients based on the observed radar reflectivities and optical thickness inferred from IR radiometer measurements.

*Atlas et al.* [1995] showed that the exponent “b” in (6) is related to the variability of the characteristic particle size, with higher size variability resulting in a lower value of “b”. Based on observed vertical distributions of ice particle size variability for which full remote sensing retrievals (as described in *Matrosov et al.* [1997]) were possible, *M99* assumes that “b” varies with height, decreasing from about 0.7 near the cloud base to about 0.6 near cloud top.

Tuning the “a” coefficient requires accurate measurement of the IR brightness temperature, which provides information about the cloud IR optical thickness,  $\tau$ , of optically thin clouds (i.e.,  $\tau \leq 3$ ) [*Matrosov et al.*, 1998]. Combining  $\tau$  and the layer-mean radar reflectivity,  $Z_m$ , the ice water path (IWP) can then be inferred [*Matrosov et al.*, 1992]. Integration of (6) over the cloud depth, with the assumption that “a” is constant with height, shows the relationship between “a”, IWP and Z to be

$$a = \frac{IWP(Z_m, \tau)}{Z(h)^{b(h)} dh}. \quad (7)$$

IWC is then calculated by substituting (7) into (6) and using the height-dependent value of b.

Ice particle characteristic size is calculated as a function of the IWC using the relationship

$$Z = GD_o^3 IWC, \quad (8)$$

where Z is in  $\text{mm}^6/\text{m}^3$ ,  $D_o$  in  $\mu\text{m}$  and IWC in

$\text{g/m}^3$ . In this relationship, the characteristic size describing the particle size distribution,  $D_o$ , is the median diameter of the equal-volume sphere and the coefficient  $G$  is a function of the particle shape, density, and size distribution [Atlas *et al.*, 1995]. By using a relationship associating particle bulk density to size [Brown and Francis, 1995],  $G$  can be related to  $D_o$  [M99] by

$$G(D_o) \approx 74 \times 10^{-6} D_o^{-1.1}. \quad (9)$$

In (9) an exponential particle size distribution and quasi-spherical particles were assumed based on a preliminary perusal of data from a 2D-C probe on the Canadian Convair 580 aircraft which flew during FIRE-ACE. The uncertainties introduced into the retrieval due to these assumptions are discussed in M99. Mean particle diameter can be calculated by substituting (9) into (8):

$$D_{mean} = 0.28 \left( \frac{Z}{74 \times 10^{-6} IWC} \right)^{1/1.9}. \quad (10)$$

The value of 0.28 is the conversion factor from  $D_o$  to mean diameter,  $D_{mean}$ , assuming an exponential particle size distribution. Matrosov *et al.* [1998] showed relative standard deviations of retrieved  $D_o$  and IWC from in situ measurements to be 30% and 55%, respectively, using techniques similar to those described above.

For these ice retrievals, since IWC and “a” are directly related, and size calculations are based on IWC, the accuracy of the technique is highly dependent on good values of “a.” There were several circumstances during the FIRE-ACE period which hindered the accurate calculation of “a” on a case-by-case basis - making the full tuned-regression technique applicable approximately 15% of the time that all-ice clouds were observed. A primary

limitation in the determination of “a” was the AERI being inoperable for a significant fraction of the time during the months of May, June and July. Although in some instances measurements from the IRT could be substituted, frequently the sky brightness temperature was below the  $-60^\circ\text{C}$  IRT detection threshold. It was also common for an upper level ice cloud to be radiometrically obscured by low level liquid clouds. Finally, it was sometimes the case that clouds were so optically thin that the uncertainty in determining “a” by the tuned regression technique became large and the accuracy of the retrieval was in question.

In cases where ice clouds were too optically thin for the tuned regression technique, no retrievals were performed. However, to expand the retrieval analysis to the ice clouds with the other limiting physical circumstances, (6) was applied with an assigned value of “a” and the same assumed form of “b.” If reasonable calculations of “a” using the tuned regression were possible for any part of a cloud, these values were extended to cover the full cloud. For cases in which no values of “a” could be calculated throughout an entire cloud, the mean “a” for the four-month period was assigned. This type of assignment leads to a larger uncertainty than the tuned regression approach provides, yet it is better than any a priori coefficient derived from clouds in non-Arctic locations. The mean “a” calculated for FIRE-ACE was  $0.095 \pm 0.067$  leading to an uncertainty of about 70% in IWC.

An ice cloud occurring over the two hour period from approximately 23:00 GMT on May 26 to 01:00 on May 27, 1998, demonstrates the ice retrieval products. This cloud was geometrically thick, but optically thin, with a base at 3 km AGL and a top near 10 km AGL. Radar reflectivity is shown in Figure 2a, retrieved IWC is shown in Figure 2b, and retrieved  $D_{mean}$  is shown in Figure 2c.

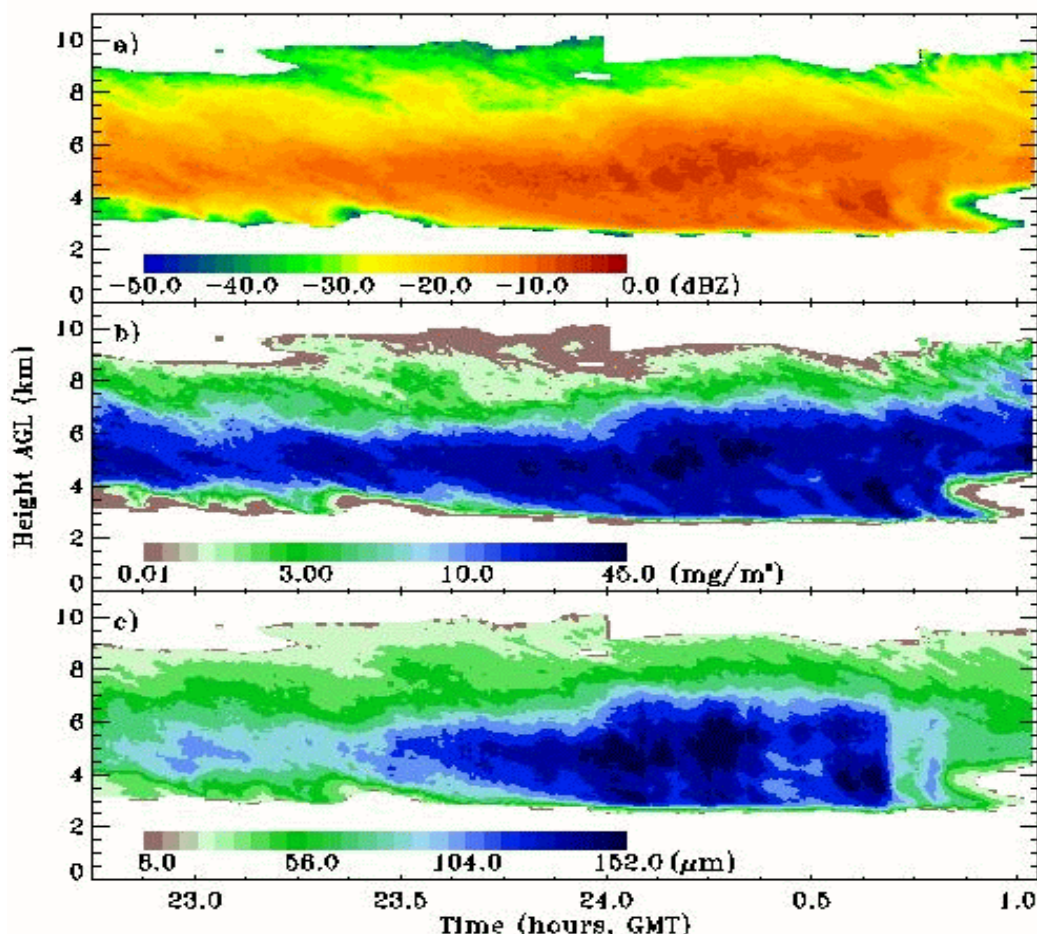


**Figure 2.** Time-height contours for May 26-27, 1998 of (a) radar reflectivity, (b) retrieved ice water content, and (c) retrieved mean particle diameter.

#### 4. Results

The cloud radar data set for the SHEBA experiment spanned nearly one year, from October 20, 1997, to October 1, 1998. This paper, however, presents statistics of cloud properties for the April through July, 1998, time period, which brackets the aircraft flights conducted during the FIRE-ACE program. Within these four months retrievals of water contents, particle characteristic sizes, and particle concentrations were calculated for clouds that appeared to be single phase - either all-ice or all-

liquid. In cases where multiple cloud layers existed, retrievals were also performed if the liquid and ice appeared to be divided into distinct layers. An example of simultaneous all-liquid and all-ice clouds occurred on June 10 (Figure 3). The liquid retrieval was applied through the depth of the low-level stratus, and (6) was applied to the upper-level ice cloud using an “a” coefficient of 0.095.

Phase determination was made on a case by case basis by examining microwave radiometer-derived LWPs, IR brightness



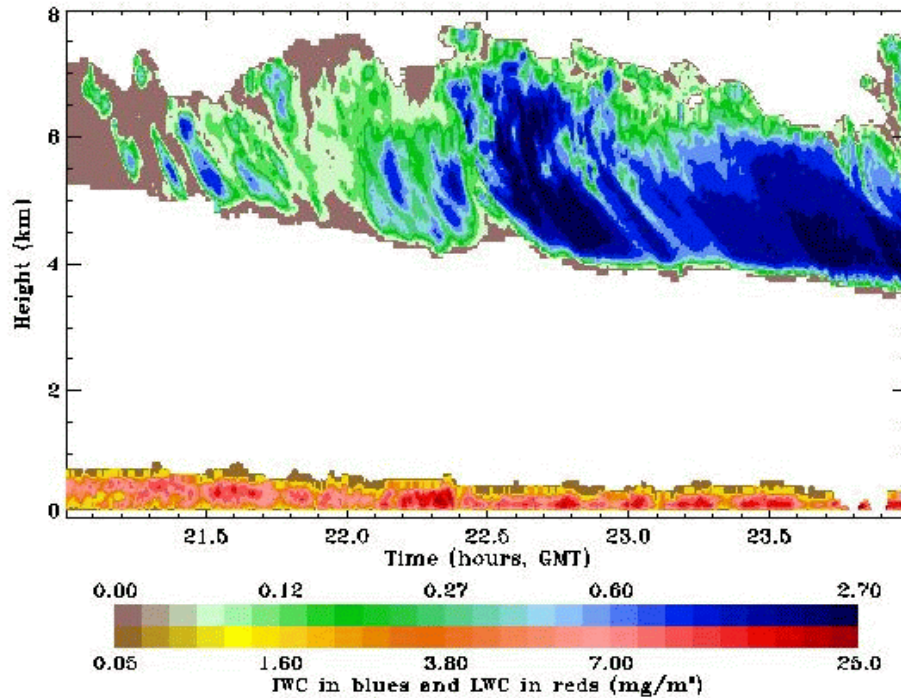


**Figure 3.** Time-height contours for June 10, 1998 of ice (blue) and liquid (red) water content.

temperatures, the structure of the radar reflectivities and Doppler velocities, lidar depolarization ratios, and temperature and humidity profiles from radiosondes. The clouds that were deemed to be single-phase generally consisted of low stratus (liquid) and mid- to upper-level cirrus (ice) clouds. The total monthly cloud fraction and the percent of observed clouds that were all-liquid or all-ice are shown in Table 1. The single phase criteria were fit approximately 34% of the time clouds were observed for the 4-month period, with all-liquid clouds occurring 17% of the time and all-ice clouds occurring 19% of the time. Note that some of the time all-liquid and all-ice clouds occurred simultaneously (<3%). There were no significant trends in the percentages of single phase clouds over the four-month period, with the exception that April had a small percentage of all-liquid clouds. Also shown in Table 1 (in parentheses) are the subset of clouds that were determined to be single-layered as well as single-

**Table 1.** Cloud type characterization, in percent of time, for the FIRE-ACE months. Fractional cloudiness is the total percentage of time clouds were observed by the radar. All other values are percentages of when clouds were present (i.e. portions of the fractional cloudiness). Single-phase cloud percentages are shown for both liquid and ice clouds. Single-phase and single-layer cloud percentages are shown in parentheses.

	<b>Fractional Cloudiness</b>	<b>All-liquid (one-layer)</b>	<b>All-ice (one-layer)</b>
April	93.1	4.2 (0.0)	21.3 (7.0)
May	88.0	23.2 (3.8)	17.6 (6.1)
June	87.8	18.4 (4.5)	23.4 (7.9)
July	93.9	23.2 (5.6)	15.0 (5.9)
Total	90.7	17.3 (3.5)	19.3 (6.7)

phased, and having a cloud base above the lowest radar range gate of 105 m.

In this section two basic types of cloud microphysical statistics are shown. The first type is the distribution of retrieved parameter values. For the sake of comparing multiple distributions, each has been normalized. The second type of result is the profile of retrieved parameters. Each retrieved profile has been normalized in cloud depth and in magnitude of the retrieved microphysical parameter - therefore mean profiles will have a maximum somewhat less than unity. To demonstrate how representative the FIRE-ACE aircraft flight days were of the entire April-July time period, retrieved parameter distributions and profiles are also shown for clouds observed on flight days although not necessarily sampled by the aircraft. These data are not to be confused with the aircraft in situ measurements.

#### 4.1. Liquid Cloud Statistics

The normalized frequency distribution of retrieved droplet effective radii for all clouds determined to be liquid during the April to July, 1998, time period is illustrated in Figure 4. The distribution shows a broad peak at 7  $\mu\text{m}$ , the minimum calculated  $R_e$  is 3  $\mu\text{m}$ , and the maximum is around 20  $\mu\text{m}$ . The mean retrieved value of  $R_e$  is 7.4  $\mu\text{m}$ , while the median value of  $R_e$  is 6.9  $\mu\text{m}$ . The median value presented here, and in the following sections, is the standard statistical median. These retrieved droplet sizes are in good agreement with liquid cloud in situ measurements made during the 1980 Arctic Stratus Experiment (ASE) [Curry *et al.*, 1996] ranging from 3.6 - 11.4  $\mu\text{m}$  with a mean of 7.5  $\mu\text{m}$ , and measurements made during the 1995 Arctic Radiation Measurements in Column Atmosphere-Surface System Experiment (ARMCAS) [Hobbs and Rangno, 1998] showing average profile  $R_e$  ranging from 3 - 12  $\mu\text{m}$ . For comparison purposes, Figure 4 also shows the

distribution of retrieved drop sizes for the seven days on which there were aircraft flights over the ice camp and all-liquid cloud layers were identified. With the exception of May 18 and July 29, most flight day cases show distributions that have slightly smaller droplet size modes than those of the April-July mean statistics. The peak of the  $R_e$  distribution for the 7 cases combined is near 5.5  $\mu\text{m}$ , the mean is 6.2  $\mu\text{m}$ , and the range of sizes is generally between 3-13  $\mu\text{m}$ .

Normalized frequency distributions of retrieved LWC for the liquid clouds which occurred during the April-July period are shown in Figure 5. The retrieved liquid water contents range from near 0 to 0.7  $\text{g}/\text{m}^3$  with a mean value of 0.1  $\text{g}/\text{m}^3$  and a median value of 0.06  $\text{g}/\text{m}^3$ . Measurements made during ASE showed a maximum measured LWC of 0.5  $\text{g}/\text{m}^3$  while those made during ARMCAS were as high as 0.66  $\text{g}/\text{m}^3$  in all-liquid clouds. Again for comparison purposes, the frequency distributions of retrieved LWC for the all-liquid clouds on seven aircraft flight days are also included. In general, the flight-day cases have distributions which are characterized by a more pronounced occurrence of LWC values in the 0.02 to 0.07  $\text{g}/\text{m}^3$  range. The mean LWC for the 7 flight-day cases is 0.08  $\text{g}/\text{m}^3$ , which is 20% smaller than the mean for the entire April-July period.

The April-July normalized distribution of retrieved liquid droplet concentrations (Figure 6) shows values ranging from 10 to 120  $\text{cm}^{-3}$  with the lower limit of 10  $\text{cm}^{-3}$  a product of the -60 dBZ limit on (5). The mean retrieved liquid droplet concentration is 54  $\text{cm}^{-3}$  and the median value is 56  $\text{cm}^{-3}$ . Measurements made during ARMCAS showed droplet concentrations that were often below 100  $\text{cm}^{-3}$ . The distributions of retrieved concentrations for the 7 flight-day cases are quite varied, however the mean distribution of these cases is similar to the April-July mean distribution, with a mean concentration of 47  $\text{cm}^{-3}$ . The smaller retrieved concentrations for

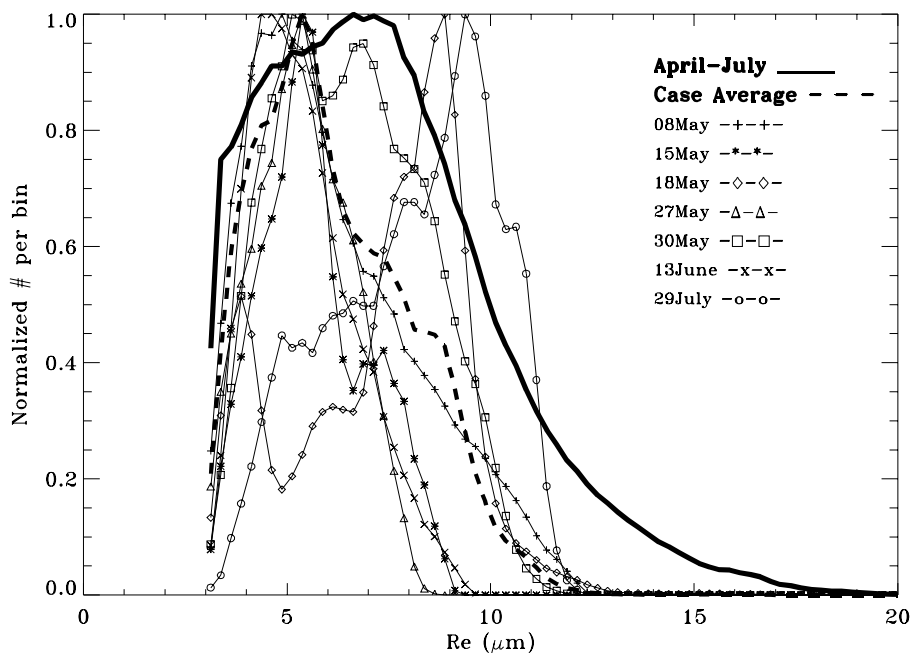


**Figure 4.** Normalized, retrieved effective radius distributions for the full April-July period (solid line) with retrieved distributions for seven flight-day liquid-cloud cases (symbols w/ lines) and the combined flight-cases average (dashed line).

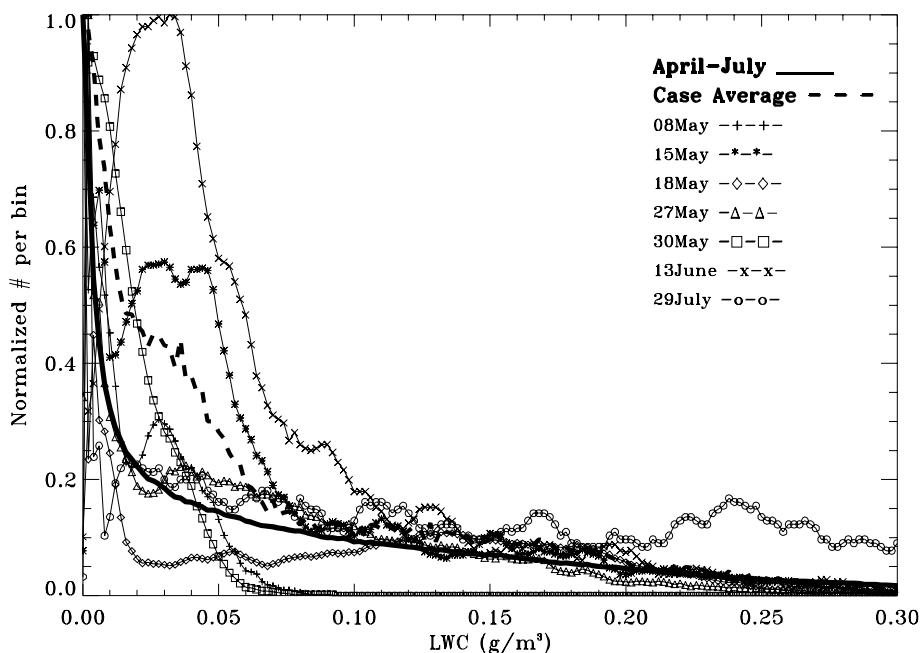


**Figure 5.** Normalized, retrieved liquid water content distributions for the full April-July period (solid line) with retrieved distributions for seven flight-day liquid-cloud cases (symbols w/ lines) and the combined flight-cases average (dashed line).

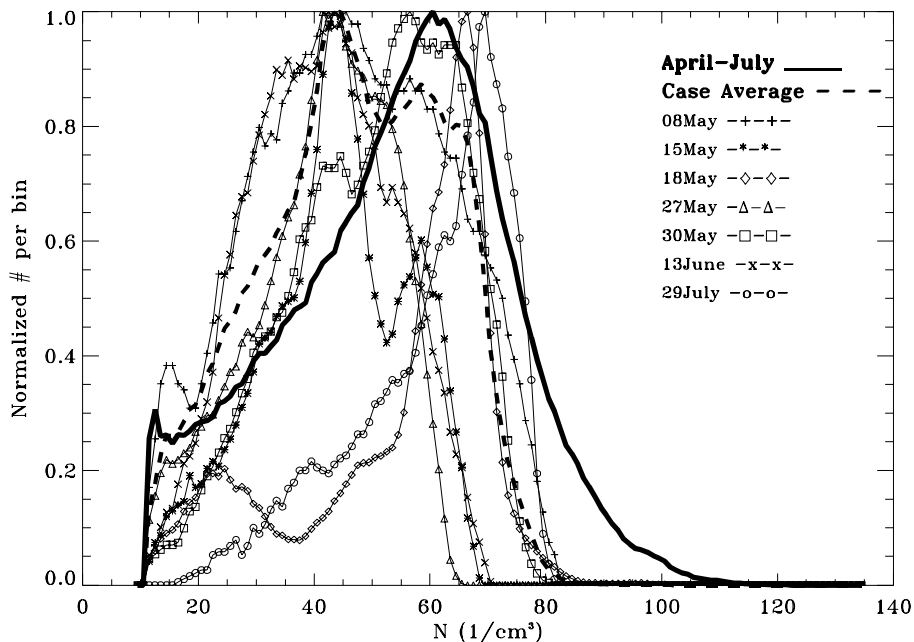


**Figure 6.** Normalized, retrieved liquid particle concentration distributions for the full April-July period (solid line) with retrieved distributions for seven flight-day liquid-cloud cases (symbols w/ lines) and the combined flight-cases average (dashed line).

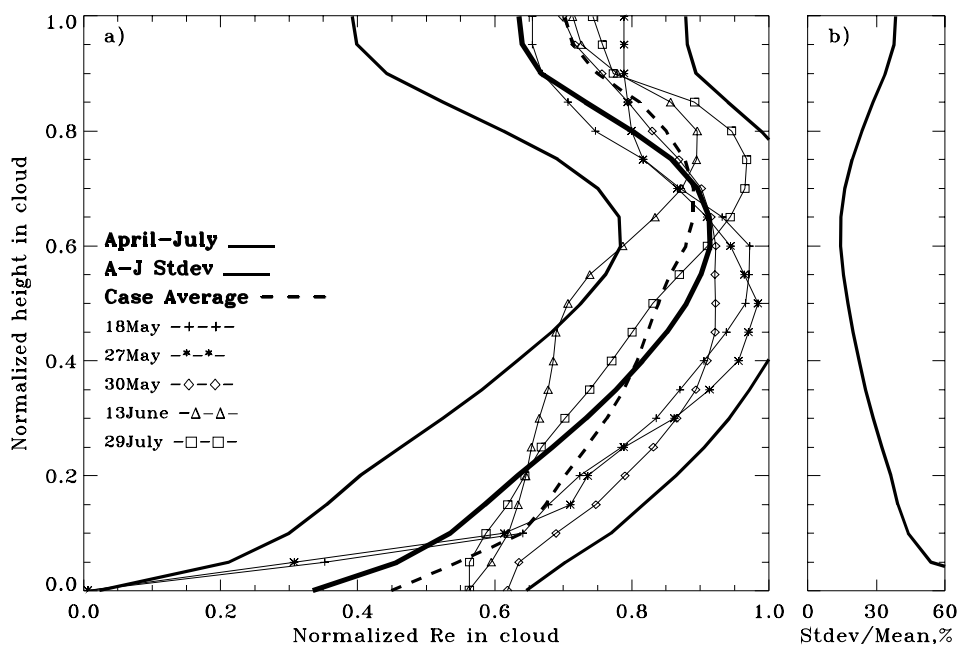


**Figure 7.** (a) Normalized, retrieved effective radius profiles for April-July (thick line), the April-July mean plus and minus the standard deviation (thin lines), five retrieved liquid-cloud flight cases (symbols w/ lines), and the average profile for the five flight-day cases (dashed line). (b) The April-July standard deviation divided by mean profile, in percent, describing the profile variability.

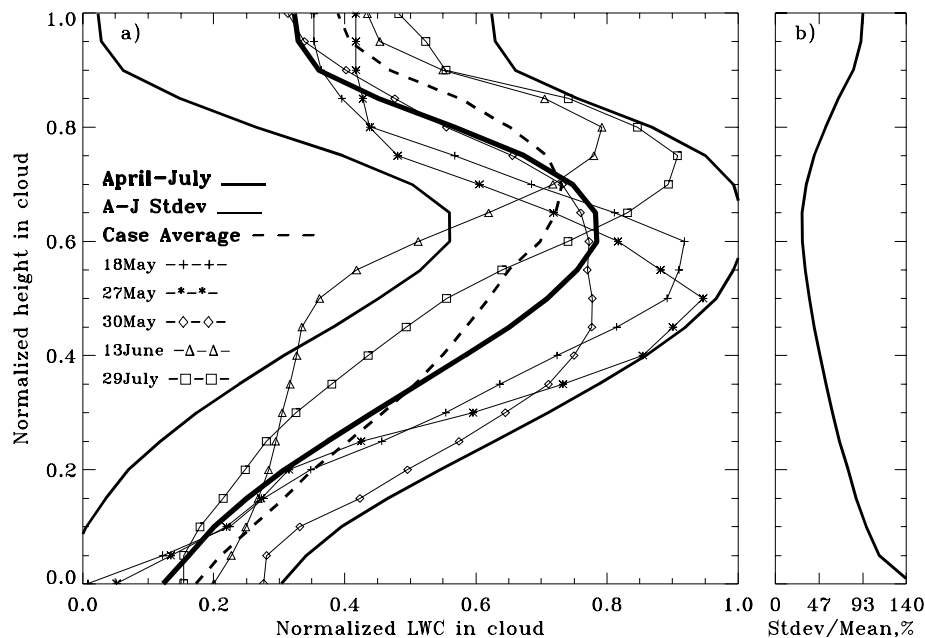


**Figure 8.** (a) Normalized, retrieved liquid water content profiles for April-July (thick line), the April-July mean plus and minus the standard deviation (thin lines), five retrieved liquid-cloud flight cases (symbols w/ lines), and the average profile for the five flight-day cases (dashed line). (b) The April-July standard deviation divided by mean profile, in percent, describing the profile variability.

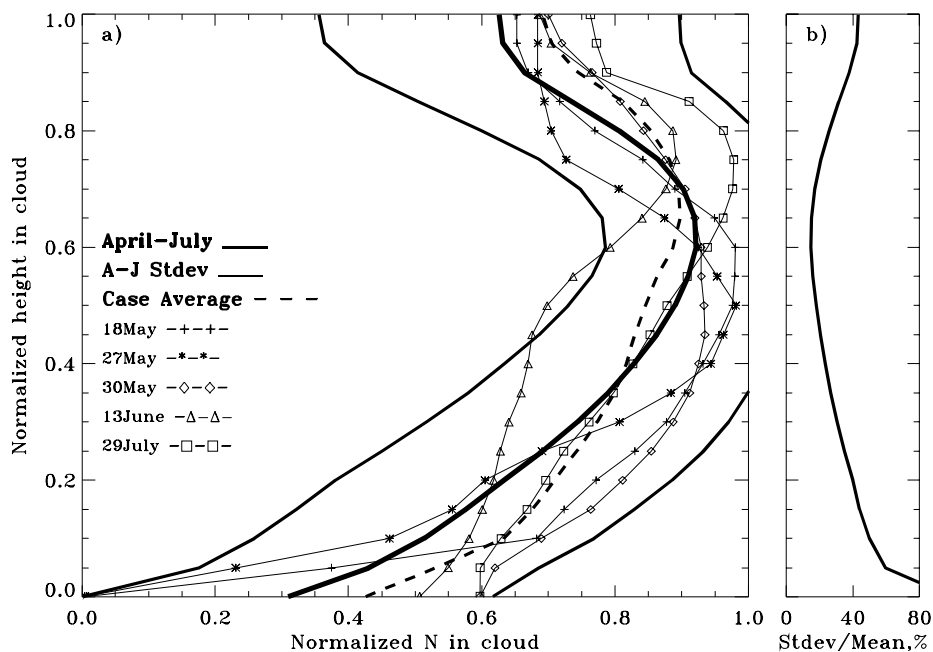


**Figure 9.** (a) Normalized, retrieved liquid particle concentration profiles for April-July (thick line), the April-July mean plus and minus the standard deviation (thin lines), five retrieved liquid-cloud flight cases (symbols w/ lines), and the average profile for the five flight-day cases (dashed line). (b) The April-July standard deviation divided by mean profile, in percent, describing the profile variability.

flight-day cases are consistent with smaller retrieved water contents and particle sizes.

For the subset of data considered to be single-layer as well as all-liquid (see Table 1), particle size profiles, normalized by cloud-depth and maximum particle size, were calculated (Figure 7a). Many of the liquid clouds observed during the April-July months had bases below the lowest radar range gate (105 m) and were therefore not useful for these profile statistics. The April-July mean profile indicates that, on average, the largest particles were found at about 3/5 of the cloud geometrical depth from the cloud base. Both above and below this level the particle sizes decreased rapidly, with the smallest particles at cloud base. The decrease in particle sizes towards the top of the cloud suggests an evaporation process occurring at cloud top. In general, the retrieved particle size profiles for the individual flight-day cases deemed to be all-liquid are within one standard deviation of the mean April-July profile. The general profile shape shows reasonable agreement with the particle size profiles from ASE, as well as with the particle size profiles calculated by *Frisch et al.* [1995] for liquid water stratus clouds measured during the 1992 Atlantic Stratocumulus Transition Experiment (ASTEX). The profile of standard deviation divided by mean (in percent), for the April-July period, which provides an estimate of the height-dependent variability from the mean, is shown in Figure 7b. The variability is generally less than 25% in the middle of the cloud, demonstrating consistency in the vertical distribution of liquid particle sizes when normalized in this manner.

Mean, normalized profiles of retrieved LWC for the single-layer, all-liquid clouds occurring in the April-July period and during the seven individual flight-day cases are presented in Figure 8a. As would be expected for a fixed concentration with height, the shape of the LWC profiles is similar to that of the particle size

profiles with the largest water contents at 3/5 of the cloud depth up from the cloud base. The variability of LWC (Figure 8b) is significantly larger (30% - 140%) than the variability of  $R_e$  (15% - 60%) due to the fact that LWC values range over three orders of magnitude while  $R_e$  only varies over one order of magnitude.

The mean, normalized profiles of retrieved liquid particle concentration (Figure 9) have shapes similar to those of droplet size and water content. Again the flight-day cases show mean retrieved profiles that are quite comparable with the mean April-July profile. The variability of the particle concentration profiles ranges from about 20% in the middle of the cloud to about 80% at the cloud base.

## 4.2. Ice Cloud Statistics

The normalized frequency distribution of retrieved ice particle mean diameters for the clouds determined to be all-ice during the April-July time period is shown in Figure 10. The distribution has a single peak at 30  $\mu\text{m}$ , with  $D_{\text{mean}}$  ranging in size from 7 to 300  $\mu\text{m}$ , a mean retrieved  $D_{\text{mean}}$  of 60  $\mu\text{m}$  and a median value of 46  $\mu\text{m}$ . A review of in situ cirrus measurements generally from lower latitudes [*Dowling and Radke, 1990*] discusses “reasonable” ice particle mean diameters of 40-70  $\mu\text{m}$  which bracket the mean retrieved FIRE-ACE value<sup>1</sup>. For comparison purposes, the frequency distributions of retrieved  $D_{\text{mean}}$  for six all-ice flight-day cases are also shown. For the flight-day cases, the distributions tend towards larger particle sizes; the distribution for the 6 cases combined has a peak at 40  $\mu\text{m}$  and a mean value of 75  $\mu\text{m}$ , both

---

<sup>1</sup> *Dowling and Radke* [1990] published actual crystal lengths which were converted to mean diameter using equations presented by *Matrosov et al.* [1995] and a range of expected aspect ratios.

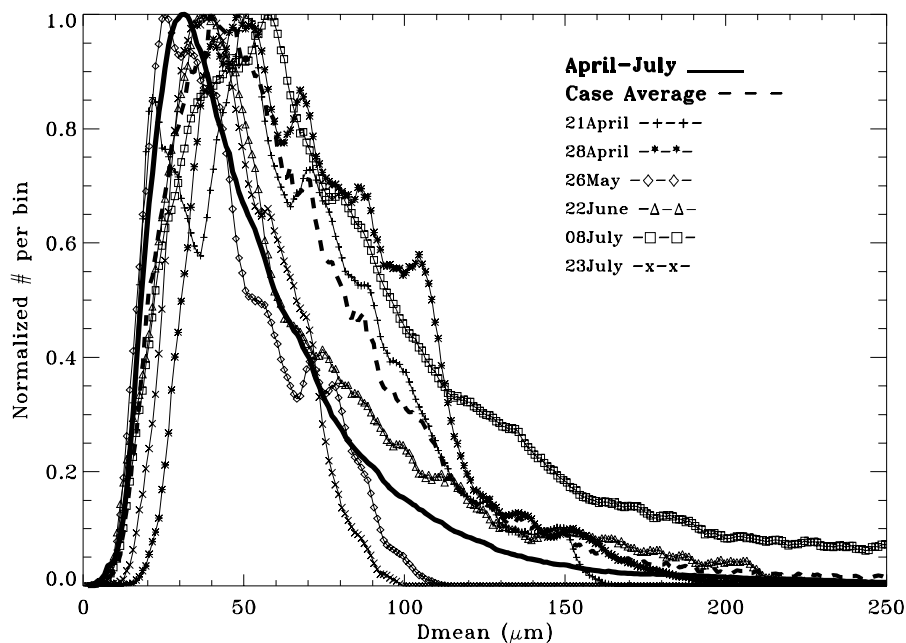


**Figure 10.** Normalized, retrieved mean particle diameter distributions for the full April-July period (solid line) with retrieved distributions for six flight-day ice-cloud cases (symbols w/ lines) and the combined flight-cases average (dashed line).

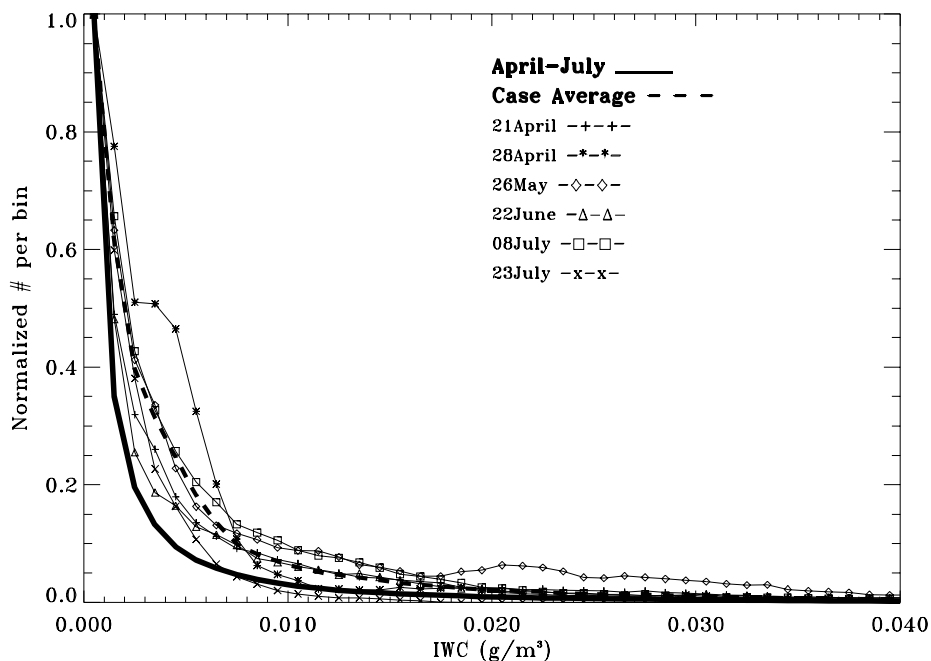


**Figure 11.** Normalized, retrieved ice water content distributions for the full April-July period (solid line) with retrieved distributions for six flight-day ice-cloud cases (symbols w/ lines) and the combined flight-cases average (dashed line).

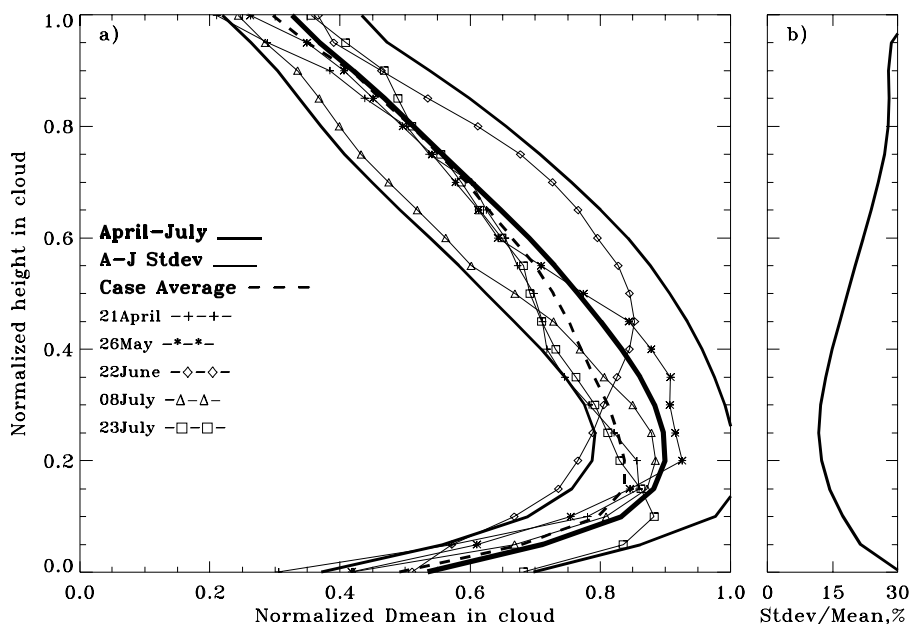


**Figure 12.** (a) Normalized, retrieved mean particle diameter profiles for April-July (thick line), the April-July mean plus and minus the standard deviation (thin lines), five retrieved ice-cloud flight cases (symbols w/ lines), and the average profile for the five flight-day cases (dashed line). (b) The April-July standard deviation divided by mean profile, in percent, describing the profile variability.

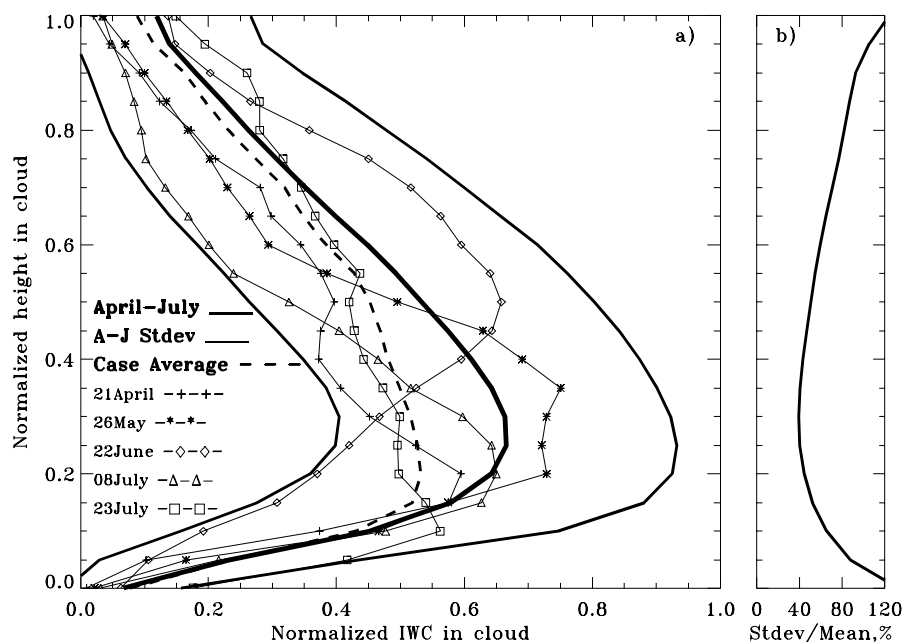


**Figure 13.** (a) Normalized, retrieved ice water content profiles for April-July (thick line), the April-July mean plus and minus the standard deviation (thin lines), five retrieved ice-cloud flight cases (symbols w/ lines), and the average profile for the five flight-day cases (dashed line). (b) The April-July standard deviation divided by mean profile, in percent, describing the profile variability.



of which are about 25% larger than the April-July values.

The normalized frequency distribution of retrieved IWC for the clouds determined to be all-ice during the April-July period is presented in Figure 11. Retrieved ice water contents range from near 0 to  $0.1 \text{ g/m}^3$  with a mean value of  $0.005 \text{ g/m}^3$  and a median value of  $0.001 \text{ g/m}^3$ . Preliminary comparisons between these ice retrievals and the in situ measurements made by the Canadian Convair 580 on April 28/29 at FIRE-ACE demonstrate good agreement, with uncertainty estimates (about 30% for  $D_{\text{mean}}$  and 60% for IWC) similar to those discussed by *Matrosov et al.* [1998]. The individual flight-day retrieved IWC distributions have shapes that are similar to the April-July distribution with the April 28 case being a slight exception, showing a larger portion of values at about  $0.003 \text{ g/m}^3$ . The mean value of retrieved IWC for the six flight-day cases is  $0.007 \text{ g/m}^3$ , which is 40% larger than the April-July mean, and is in agreement with the larger than average particle sizes retrieved during the aircraft flight times.

Normalized profiles of retrieved mean particle diameter were calculated for the single-layer, all-ice, clouds in the same manner as described for the liquid cloud retrievals (Figure 12a). The average April-July profile shows the largest particles at 1/5th of the cloud depth from the cloud base, with steady particle growth from the top down to this level, and rapid sublimation below this level to the cloud base. All five of the individual flight-day mean retrieved profiles are similar in shape to the April-July profile, and generally remain within one standard deviation of the four-month average. The vertical distributions of ice particle size observed here are in good agreement with the vertical distributions presented in *Matrosov* [1997] for ice clouds measured in Kansas, the Madeira Islands, and Arizona. The height-dependent variability is generally smaller than 30% (Figure 12b),

demonstrating consistency in the vertical distribution of retrieved particle sizes.

The corresponding, normalized IWC profiles for single-layer, all-ice, clouds are shown in Figure 13. As with liquid clouds, the vertical distributions of retrieved water content and particle size in ice clouds have similar shapes, demonstrating the direct relationship between these two parameters. The height-dependent variability of retrieved IWC values is much larger than that of mean particle diameter, again because IWC values range over four orders of magnitude while mean diameters generally range over two orders of magnitude.

## 5. Summary and Future Work

A suite of remote-sensing, cloud microphysics retrieval techniques was applied to ground-based radar and radiometer measurements made during the months of April through July, 1998, as part of the FIRE-ACE and SHEBA programs. The techniques, which are summarized in this paper, were applied to all clouds determined to be of a single phase, i.e., all-ice or all-liquid. The application of these techniques has led to the compilation of a unique and large set of retrieved microphysics data for the Arctic Ocean region. Retrieved parameter ranges, means and medians covering the full four-month FIRE-ACE period are summarized in Table 2.

Generally, the retrieved liquid-cloud parameter values are in good agreement with previous in situ measurements made in the Arctic [*Curry et al.*, 1996; *Hobbs and Rangno*, 1998]. Liquid-cloud particle size, water content, and concentration increased from the cloud base to about 3/5 of the cloud geometrical depth from the base, then decreased up to the cloud top. The shape of these retrieved profiles is in reasonable agreement with stratus cloud profiles presented in the literature [*Curry*, 1986; *Frisch et al.*, 1995] and the relatively low variability of these profiles

**Table 2.** Range, mean, and median for each retrieved parameter. Retrieved ranges are based on 99.9% of the data in order to remove extreme outliers.

Parameter	Range	Mean	Median
$R_e$ [ $\mu\text{m}$ ] (liquid)	3-20	7.4	6.9
LWC [ $\text{g}/\text{m}^3$ ] (liquid)	0-0.7	0.1	0.06
N [ $\text{cm}^{-3}$ ] (liquid)	10-120	54	56
$D_{\text{mean}}$ [ $\mu\text{m}$ ] (ice)	7-300	60	46
IWC [ $\text{g}/\text{m}^3$ ] (ice)	0-0.1	0.005	0.001

show consistency over the full four-month period. The retrieved values of liquid water content are linearly related to the microwave radiometer-derived liquid water path, which, due to differing models for the dielectric constants of water, has an uncertainty of 15-25% for super-cooled liquid clouds.

Retrieved ice cloud particle sizes and water contents show decent agreement in preliminary comparisons with in situ measurements made at FIRE-ACE. Normalized profiles of these retrieved microphysical parameters demonstrate that in ice clouds mean particle diameter and ice water content increase sharply from the cloud base to 1/5 of the cloud geometrical depth from the base, and then decrease up to the cloud top. This profile shape is similar to the vertical profiles presented by *Matrosov* [1997]. In the future, more in depth case study comparisons, both for all-ice and all-liquid clouds, will be made between the retrieved parameters presented here and in situ measurements made during FIRE-ACE.

This study also assesses how representative the single-phase clouds on individual FIRE-ACE flight days were of the April-July time period in general. These results are summarized in Table 3. Generally, the all-liquid clouds occurring on flight days showed smaller retrieved droplet effective radii, liquid water contents and concentrations than the April-July mean values by about 16%, 20%, and 13%, respectively. The opposite was observed for the flight days containing all-ice clouds. Flight-day retrieved ice particle mean diameters were about 25% larger than the April-July mean value and ice water contents were 40% larger. Vertical distributions of all ice and liquid parameters through the cloud depth show that the flight-day retrieval cases were generally within one standard deviation of the April-July mean retrieved profiles. Aircraft flight data should be

**Table 3.** Mean retrieved microphysical parameters for the full April-July time period and for the flight-day cases during those months (including the percentage difference of the flight-day case mean from the April-July mean).

Parameter	April- July Mean	Flight-day Case Means	Percent Different
$R_e$ [ $\mu\text{m}$ ] (liquid)	7.4	6.2	16 %
LWC [ $\text{g}/\text{m}^3$ ] (liquid)	0.1	0.08	20 %
N [ $\text{cm}^{-3}$ ] (liquid)	54	47	13 %
$D_{\text{mean}}$ [ $\mu\text{m}$ ] (ice)	60	75	25 %
IWC [ $\text{g}/\text{m}^3$ ] (ice)	0.005	0.007	40 %

interpreted in view of the fact that *Minnis et al.* [this issue] have shown diurnal variations in cloud properties and all aircraft flights took place between approximately 20:00 and 01:00 GMT.

The single-phase condition limited the retrieval techniques presented here to about 34% of the time clouds occurred during the April-July period. Application of these retrieval techniques, or hybridizations thereof, to mixed-phase clouds will likely be less successful [*Hobbs et al.*, this issue]. New techniques are, however, being developed that may allow for the retrieval of ice parameters in mixed phase clouds by using only radar reflectivity and Doppler velocity measurements. All of the retrieval techniques presented here will in the near future be applied to the full SHEBA year of radar and radiometer data.

**Acknowledgements.** This work was supported by the NASA FIRE-ACE program under contract # L64205D, the NSF SHEBA program under agreement # OPP-9701730 and the NASA EOS Validation Program under contract # S-97895-F. We would like to thank the program managers Bob Curran, Michael Ledbetter and David O'C Starr, respectively. Contributions by S. Frisch were supported by interagency agreement #DE-A103-97ER62342/A002 with the U. S. Department of Energy (DOE). Microwave and IR radiometer data were obtained from the Atmospheric Radiation Measurement Program sponsored by the DOE. Aircraft data were obtained from the University of Washington Cloud and Aerosol Research Group's (CARG) Convair-580 research aircraft under the scientific direction of Peter Hobbs, and the NCAR Research Aviation Facility's C-130 research aircraft. The CARG's participation in this study was supported by NSF grant OPP-9808163 and NASA grants NAG-1-2079 and NCC5-326. Radiosonde data were obtained from the SHEBA Project Office at the University of Washington,

Applied Physics Laboratory (UW/APL). Duane Hazen and Wendi Madsen, of NOAA/ETL provided the engineering and programming expertise for the cloud radar. The logistics of deployment at the SHEBA site was greatly aided by the efforts of Kevin Widener and Bernie Zak of the DOE/ARM Program. We would like to thank ETL scientists Jeffrey Otten, Janet Intrieri and Ann Keane who spent many weeks at the SHEBA ice camp monitoring radar operations. Finally, the collection of these valuable, year-long datasets would not have been possible without the support of the SHEBA logistics team from UW/APL, and the crew of the Canadian Coast Guard Ship Des Grosseilliers.

## References

- Atlas, D., S. Y. Matrosov, A. J. Heymsfield, M.-D. Chou, and D. B. Wolff, Radar and radiation properties of ice clouds, *J. Appl. Meteor.*, *34*, 2329-2345, 1995.
- Brown, P. R. A., and P.N. Francis, Improved measurements of the ice water content in cirrus using a total-water probe, *J. Atmos. Oceanic Technol.*, *12*, 410-414, 1995.
- Curry, J. A., et al., FIRE Arctic Clouds Experiment, *Bull. Amer. Meteorol. Soc.*, *81*, 5-29, 2000.
- Curry, J. A., W. B. Rossow, D. Randall, J. L. Schramm, Overview of Arctic cloud and radiation characteristics, *Bull. Amer. Meteor. Soc.*, *9*, 1721-1764, 1996.
- Curry, J. A., and E. E. Ebert, Annual cycle of radiation fluxes over the Arctic Ocean: Sensitivity to cloud optical properties, *J. Climate*, *5*, 1267-1280, 1992.

- Curry, J. A., Interactions among turbulence, radiation and microphysics in Arctic stratus clouds, *J. Atmos. Sci.*, *43*, 90-106, 1986.
- Dowling, D. R., and L. R. Radke, A summary of the physical properties of cirrus clouds, *J. Appl. Meteor.*, *29*, 970-978, 1990.
- Frisch, A. S., I. Djalalova, G. Feingold, and M. Poellot, On the retrieval of effective radius with cloud radars, *J. Geophys. Res.*, submitted. (Referred to as 2000a in text)
- Frisch, A. S., B. E. Martner, I. Djalalova, M. R. Poellot, Comparison of radar/radiometer retrievals of stratus cloud liquid-water content profiles with in situ measurements by aircraft, *J. Geophys. Res.*, accepted. (Referred to as 2000b in text)
- Frisch, A. S., G. Feingold, C. W. Fairall, T. Uttal, and J. B. Snider, On cloud radar and microwave radiometer measurements of stratus cloud liquid water profiles, *J. Geophys. Res.*, *103*, 23,195-23,197, 1998.
- Frisch, A. S., C. W. Fairall, and J. B. Snider, Measurements of stratus cloud and drizzle parameters in ASTEX with a Ka-band Doppler radar and microwave radiometer, *J. Atmos. Sci.*, *52*, 2788-2799, 1995.
- Hobbs, P. V., A. L. Rangno, T. Uttal, M. D. Shupe, Airborne studies of cloud structures over the Arctic Ocean and comparisons with deductions from ship-based 35 Ghs radar measurements, *J. Geophys. Res.*, this issue.
- Hobbs, P. V., and A. L. Rangno, Microstructures of low and middle-level clouds over the Beaufort Sea, *Q. J. R. Meteorol. Soc.*, *124*, 2035-2071, 1998.
- Intrieri, J. M., M. D. Shupe, T. Uttal, B. J. McCarty, Annual cycle of Arctic cloud geometry and phase from radar and lidar at SHEBA, *J. Geophys. Res.*, submitted. (Referred to as 2000 in text).
- Liao, L. and K. Sassen, Investigation of relationships between Ka-band radar reflectivity and ice and liquid water content, *Atmos. Res.*, *34*, 231-248, 1994.
- Mace, G. G., T. P. Ackerman, P. Minnis, and D. F. Young, Cirrus layer microphysical properties derived from surface-based millimeter radar and infrared interferometer data, *J. Geophys. Res.*, *103*, 23,207-23,216, 1998.
- Matrosov, S. Y., Retrievals of vertical profiles of ice cloud microphysics from radar and IR measurements using tuned regressions between reflectivity and cloud parameters, *J. Geophys. Res.*, *104*, 16,741-16,753, 1999.
- Matrosov, S. Y., A. J. Heymsfield, R. A. Kropfli, B. E. Martner, R. F. Reinking, J. B. Snider, P. Piironen, and E. W. Eloranta, Comparisons of ice cloud parameters obtained by combined remote sensor retrievals and direct methods, *J. Atmos. Oceanic Technol.*, *15*, 184-196, 1998.
- Matrosov, S. Y., Variability of microphysical parameters in high-altitude ice clouds: Results of the remote sensing method, *J. Appl. Meteorol.*, *36*, 633-648, 1997.
- Matrosov, S. Y., A. J. Heymsfield, J. M. Intrieri, B. W. Orr, and J. B. Snider, Ground-based remote sensing of cloud particle sizes during the 26 November 1991 FIRE-II cirrus case: Comparisons with in situ data, *J. Atmos. Sci.*, *52*, 4128-4142, 1995.

- Matrosov, S. Y., B. W. Orr, R. A. Kropfli, and J. B. Snider, Retrievals of vertical profiles of cirrus cloud microphysical parameters from Doppler radar and infrared radiometer measurements, *J. Appl. Meteorol.*, 33, 617-626, 1994.
- Matrosov, S. Y., T. Uttal, J. B. Snider, and R. A. Kropfli, Estimation of ice cloud parameters from ground-based infrared radiometer and radar measurements, *J. Geophys. Res.*, 97, 11,567-11,574, 1992.
- Minnis, P., D. R. Doelling, V. Chakrapani, D. C. Spangenberg, L. Nguyen, R. Palikonda, T. Uttal, M. Shupe, R. F. Arduini, Cloud coverage during FIRE ACE derived from AVHRR data, *J. Geophys. Res.*, this issue.
- Moran, K. P., B. E. Martner, M. J. Post, R. A. Kropfli, D. C. Welsh, and K. B. Widener, An unattended cloud-profiling radar for use in climate research, *Bull. Am. Meteorol. Soc.*, 79, 443-455, 1998.
- Perovich, D. K., et al., Year on ice gives climate insights, *EOS, Transactions, American Geophysical Union*, 80, 481 & 485-486, 1999.
- Revercomb, H., F. A. Best, R. G. Dedecker, R. P. Dirks, R. A. Herbsleb, R. O. Knuteson, J. F. Short, and W. L. Smith, Atmospheric Emitted Radiance Interferometer (AERI) for ARM. Preprints. *Fourth Symp. on Global Change Studies*, Amer. Meteor. Soc., Anaheim, CA, pp. 46-49, 1993.
- Rossow, W. B., A. W. Walker, and L. C. Garder, Comparison of ISCCP and other cloud amounts, *J. Climate*, 6, 2394-2418, 1993.
- Sassen, K., G. G. Mace, Z. Wang, M. R. Poellot, S. M. Sekelsky, and R. E. McIntosh, Continental stratus clouds: A case study using coordinated remote sensing and aircraft measurements, *J. Atmos. Sci.*, 56, 2345-2358, 1999.
- Sassen, K., and L. Liao, Estimation of cloud content by W-band radar, *J. Appl. Meteorol.*, 35, 2705-2706, 1996.
- Sassen, K., Ice cloud content from radar reflectivity, *J. Climate Appl. Meteor.*, 26, 1050-1053, 1987.
- Stephens, G. L., S.-C. Tsay, P. W. Stackhouse, Jr. and P. J. Flatau, The relevance of the microphysical and radiative properties of cirrus clouds to climate and climatic feedback, *J. Atmos. Sci.*, 47, 1742-1753, 1990.
- Uttal, T., et al., Surface Heat Budget of the Arctic, *Bull. Amer. Meteorol. Soc.*, submitted. (Referred to as 2000 in text)